

Quantum-Acoustical Drude Peak Shift

Joonas Keski-Rahkonen^{1,2,*} Xiaoyu Ouyang^{3,4} Shaobing Yuan⁴ Anton M. Graf⁵
 Alhun Aydin^{1,6} and Eric J. Heller^{1,2}

¹Department of Physics, Harvard University, Harvard University, Cambridge, Massachusetts 02138, USA

²Department of Chemistry and Chemical Biology, Harvard University, Cambridge, Massachusetts 02138, USA

³Yuanpei College, Peking University, No. 5 Yiheyuan Road, Beijing 100871, China

⁴School of Physics, Peking University, No. 5 Yiheyuan Road, Beijing 100871, China

⁵Harvard John A. Paulson School of Engineering and Applied Sciences, Harvard, Cambridge, Massachusetts 02138, USA

⁶Faculty of Engineering and Natural Sciences, Sabanci University, 34956 Tuzla, Istanbul, Türkiye



(Received 15 November 2023; accepted 18 March 2024; published 3 May 2024)

Quantum acoustics—a recently developed framework parallel to quantum optics—establishes a non-perturbative and coherent treatment of the electron-phonon interaction in real space. The quantum-acoustical representation reveals a displaced Drude peak hiding in plain sight within the venerable Fröhlich model: the optical conductivity exhibits a finite frequency maximum in the far-infrared range and the dc conductivity is suppressed. Our results elucidate the origin of the high-temperature absorption peaks in strange or bad metals, revealing that dynamical lattice disorder steers the system towards a non-Drude behavior.

DOI: 10.1103/PhysRevLett.132.186303

Stretching over four decades, an intensive theoretical pursuit has concentrated on finding an all-embracing explanation for a plethora of puzzling phenomena which have been colloquially labeled as “bad” or “strange.” These kinds of “bizarre” materials seem to defy the traditional paradigms for electron behavior [1] in metals. Mysteries abound, such as high-temperature superconductivity beyond the grasp of the BCS theory [2,3], the paradoxical existence of pseudogaps [4–8] and charge density waves [9–12], the violation of the Mott-Ioffe-Regel (MIR) limit [13,14], not to mention the major dilemma of linear-in-temperature resistivity over a wide temperature range (see, e.g., Refs. [15–21]) at the mysterious but ubiquitous Planckian bound [22]. This list of theoretical challenges also includes the elusive emergence of displaced Drude peaks (DDP) [23–37]: a prominent absorption peak located typically in the infrared range, signaling a breakdown of the conventional Drude picture. This Letter reveals the origin of this phenomenon as the result of strong electron-phonon interaction if treated correctly as nonperturbative and coherent.

A putative culprit for the observed Drude shift in the optical conductivity peak has been suggested to be some as yet unidentified dynamical disorder that generates evanescent localization, thus hampering but not precluding charge carrier diffusion [38–42]; Consequently, the zero-frequency conductivity does not vanish completely, but it is strongly suppressed, favoring the DDP phenomenology. This scenario contrasts with alternative points of view, like the common arguments resorting to collective modes [43,44] or to strong electron-electron correlations [45,46].

Here we show that a morphing potential landscape of hills and valleys stemming from thermal lattice vibrations

by the Fröhlich Hamiltonian (see Ref. [47]), as illustrated in Fig. 1 is the sought-after sea of “slowly moving bosonic impurities” [41], or the cryptic “self-induced randomness” [42,48]. In a broader milieu, the subtle interplay between the Anderson localization and lattice vibrations has been encountered in a wide class of random metal alloys and other degenerate disordered systems. In fact, the intricate game of being localized or not was identified early on by Gogolin *et al.* [49,50] and Thouless [51], even pondered by Anderson himself [52,53].

The random fluctuations introduced by lattice motion slowly but surely scramble the quantum interference required for localization of the electronic state, resulting in *transient* localization (for capturing the essential aspects of this phenomenon, see, e.g., Ref. [54]), which has lately

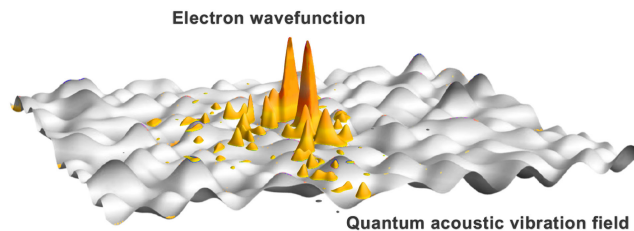


FIG. 1. Quantum acoustics. Illustration of the coherent state lattice vibrations at a certain temperature. Electrons experience a spatially continuous internal field formed by the thermal acoustic distortions. While undergoing quasielastic scattering events, like due to impurities, electrons can also be incipiently trapped by valleys of slowly undulating and propagating deformation potential when their kinetic energy is comparable to the fluctuations of the deformation potential.

been of interest in the context of crystalline organic semiconductors [55,56] and halide perovskites [57].

The quantum-acoustic route to linear and universal resistivity in strange metals [58] has opened up a new path unrelated to quantum criticality [59,60], and not relying on (strong) electron-electron interaction [48,61], instead starting with the standard Fröhlich Hamiltonian.

Following the path paved in Refs. [47,58], here we demonstrate the formation of a DDP due to the electrons interacting with fluctuating lattice degrees of freedom. We go further by showing that this mechanism gives rise to a temperature dependence of spectral features in agreement with experimental DDP observations in strange metals.

More specifically, we consider the following Fröhlich Hamiltonian [62,63] describing the lowest-order (linear) lattice-electron coupling [64]:

$$\mathcal{H}_F = \sum_{\mathbf{p}} \varepsilon_{\mathbf{p}} c_{\mathbf{p}} c_{\mathbf{p}}^{\dagger} + \sum_{\mathbf{q}} \hbar \omega_{\mathbf{q}} a_{\mathbf{q}}^{\dagger} a_{\mathbf{q}} + \sum_{\mathbf{p}\mathbf{q}} g_{\mathbf{q}} c_{\mathbf{p}+\mathbf{q}}^{\dagger} c_{\mathbf{p}} (a_{\mathbf{q}} + a_{-\mathbf{q}}^{\dagger}), \quad (1)$$

where $c_{\mathbf{p}}$ ($c_{\mathbf{p}}^{\dagger}$) is the creation (annihilation) operator for electrons with momentum \mathbf{p} and energy $\varepsilon_{\mathbf{p}}$; whereas $a_{\mathbf{q}}$ ($a_{\mathbf{q}}^{\dagger}$) is the creation (annihilation) operator for longitudinal acoustic phonons of wave vector \mathbf{q} and energy $\hbar \omega_{\mathbf{q}}$, respectively. The electron-phonon interaction is defined by its Fourier components $g_{\mathbf{q}}$. By following the steps of the recently established coherent state formalism in Ref. [47], the Hamiltonian gives rise to an undulating and propagating potential landscape (Supplemental Material, Sec. I [65]):

$$V_D(\mathbf{r}, t) = \sum_{\mathbf{q}}^{|q| \leq q_D} g_{\mathbf{q}} \sqrt{\langle n_{\mathbf{q}} \rangle_{\text{th}}} \cos(\mathbf{q} \cdot \mathbf{r} - \omega_{\mathbf{q}} t + \varphi_{\mathbf{q}}), \quad (2)$$

where q_D is Debye wave number defining the Debye frequency ω_D , \mathbf{r} is continuous position, $\varphi_{\mathbf{q}} = \arg(\alpha_{\mathbf{q}})$ is the (random) phase of a coherent state $|\alpha_{\mathbf{q}}\rangle$, and the mode population is determined by $\langle n_{\mathbf{q}} \rangle_{\text{th}}$.

The coherent state picture developed here is the dual partner of the traditional number state description of electron-lattice dynamics, so widely successful for describing electron resistivity [75]. In addition to recovering the results of the conventional Bloch-Grüneisen theory [76,77], the coherent state representation extends beyond perturbation theory (see Ref. [47] for a more detailed discussion). The coherent state limit of quantum acoustics reveals a real-space, time-dependent description of electron-lattice interaction. A very similar notion was introduced in 1957 by Hanbury Brown and Twiss for the vector potential of a blackbody field [78], with the essential difference of missing the ultraviolet cutoff, i.e., the Debye wave number in the definition of our deformation potential originating from the minimal lattice spacing.

This follows the quantum optics pathway pioneered by Glauber [79], a long neglected but essential wave perspective for lattice vibrations—*quantum acoustics*. Bardeen and Shockley, in the 1950s, regarded dynamical lattice distortions in nonpolar semiconductors [80,81], and it seemed they would have been happy with a coherent state description, but the theory was subsumed by a number state, perturbative perspective.

Within the present deformation potential framework, an electron undergoes quasielastic, coherence-preserving scattering events when roaming through the slowly altering potential landscape of hills and valleys.

In this work, we focus on three prototypical compounds classified as strange or bad metals, namely, LSCO, Bi2212, and $\text{Sr}_3\text{Ru}_2\text{O}_7$ (Supplemental Material, Sec. II [65]). However, we want to stress that the physics we find below transcends the material-specific constraints: In general, dynamical disorder, caused by lattice vibrations here, temporarily confines electrons to nest in its instantaneous potential wells (see Fig. 1, a hallmark of transient localization dynamics, resulting in the buildup of a DDP).

It appears that, regarding photoabsorption, electrons are insensitive to the lattice dynamics when $\omega \gg \omega_D$. In other words, the deformation landscape appears as if it is stationary for an electron in this regime, a notion confirmed by our results below.

Motivated by this, we initially freeze the potential and study its transitory electronic eigenstates. Since the allowed transitions take place near the Fermi level, we are allowed to focus on the states lying within the stack of $\varepsilon_F \pm 3k_B T$. Figure 2 shows examples of eigenstates for the three materials at different temperatures along with the

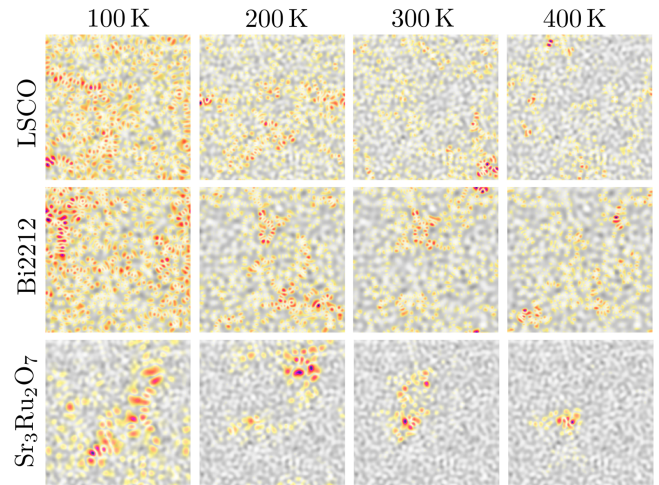


FIG. 2. Transient localized states. A selection of eigenstates (red color scheme) near the Fermi level is shown for the considered prototype materials at four temperatures, where the gray scale represents the corresponding frozen deformation potential. An increasing temperature leads to more spatially confined states that are linked to fugitive, Anderson-localized states in transient dynamics.

profile of the deformation potential. Despite the diversity among the physical settings, all three materials share similar qualitative characteristics: Instead of being spatially extended, as observed at lower temperatures ($E_F/V_{\text{rms}} \gtrsim 1$), the relevant states appear to be localized in the dips of the potential at temperatures $E_F/V_{\text{rms}} \lesssim 1$ where the potential fluctuation V_{rms} is comparable to Fermi energy E_F . These eigenstates of the frozen potential relate to the localized states associated with the transient dynamics.

Next, we compute the corresponding optical conductivity $\sigma(\hbar\omega)$ within the Kubo formalism first by numerically diagonalizing the Hamiltonian with the potential given in Eq. (2) (see Supplemental Material, Sec. III [65]). In the upper panel of Fig. 3, we present the optical conductivity at various temperatures for the three chosen materials, averaged over an ensemble of 100 random realizations of the deformation potential. With increasing temperature, the optical conductivity evolves from the Drude-peak behavior of having a sharp maximum value located at $\omega = 0$ into a displaced peak: the maximum conductivity point steadily shifts towards higher energies $\hbar\omega$ and the conductivity peak profile broadens.

In addition, we show the temperature dependence of the peak locations and their width in Fig. 4. We determine the peak location $\hbar\omega_p$ as the energy at which the optical

conductivity $\sigma(\hbar\omega)$ reaches its maximum. The peak width $\hbar\Delta\omega_p$ is then defined in a similar manner as in Ref. [82]: the distance between the maximum and the optical conductivity point in the high-energy tail where the height of the maximum is dropped by 50%. Figure 4 further confirms and quantifies the migration and broadening of the DDP with increasing temperature present in Fig. 3.

To further validate the frozen potential results above, we expand our DDP analysis by computing the optical conductivity while considering the temporal evolution of the deformation potential. Nonetheless, we can still determine the conductivity $\sigma(\hbar\omega)$ by utilizing the Kubo formalism (see Supplemental Material, Sec. IV [65]). In short, we take advantage of the already defined eigenstates of the frozen deformation potentials as initial conditions, and let it thereafter unfold according to Eq. (2).

The lower panel of Fig. 3 shows the optical conductivity spectrum of the three materials at different temperatures in the case of a dynamical potential field, averaged over 10 realizations of the distorted potential landscape. As expected, the dynamical conductivity spectrum deviates from the frozen potential prediction when $\omega \lesssim \omega_D$ is indicated by the black dash line in Fig. 3. Instead of strong suppression near to the dc conductivity as in the static landscape situation, we observe a saturation of the optical conductivity within an energy window of the order of

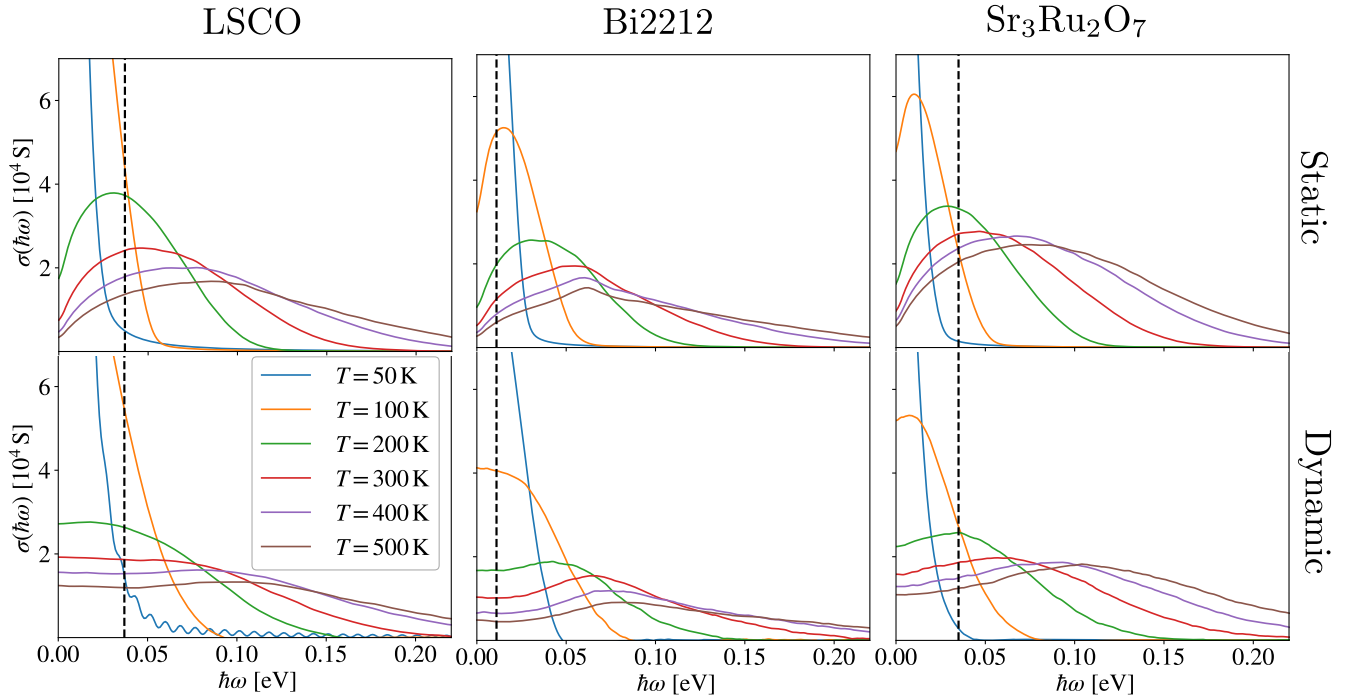


FIG. 3. Frozen versus dynamical quantum acoustic vibration field. The upper and lower panels display the optical conductivity for the three materials at different temperatures, resolved within the static and dynamical potential landscapes averaged over 100 and 10 realizations, respectively. The back dashed line marks the Debye frequency of the given material below which the frozen potential assumption breaks down. A key dynamical effect is the saturation of conductivity in the regime $\omega \lesssim \omega_D$, instead of the suppression evident in the static case. However, regardless of the deformation potential dynamics and the chosen material, the optical conductivity peak shifts from the Drude-peak edict of situating at $\omega = 0$ to higher energies and broadens as the temperature increases.

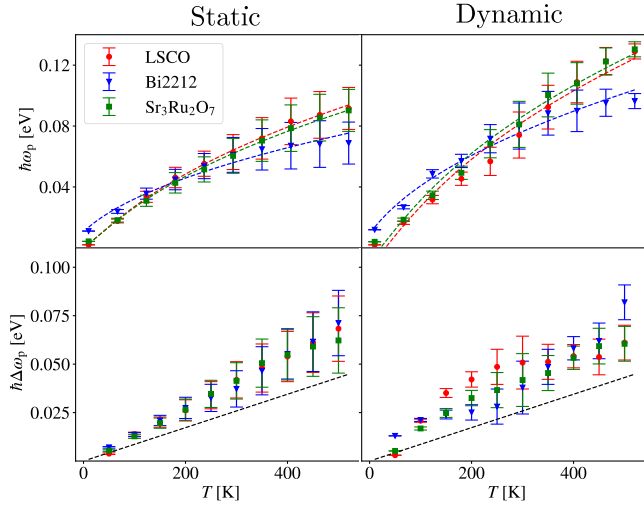


FIG. 4. Position and width of the Drude peak. The panels show the mean location (top) and width (bottom) of the optical conductivity peak as a function of temperature for the studied materials, averaged over 100 (static) and 10 (dynamic) deformation potential realizations, with error bars representing the standard deviation within the given ensemble. Specifically, as the temperature increases, there is a generic upward shift in the Drude peaks towards higher energies (upper panel), accompanied by a broadening of the peaks (lower panel). Colored dashed curves show the fittings for the DDP location estimated with the assumption that it is mostly determined by the strength of the deformation potential ($\hbar\omega_p \propto V_{\text{rms}}$). Furthermore, the width of the DDPs live near to Planckian bound ($\hbar\Delta\omega_p \sim k_B T$), which is indicated by the black dashed line.

0.1 eV near the zero frequency. This can be interpreted as the reversed adiabatic approximation where the external electric field of frequency $\omega \ll \omega_D$ is a slow varying degree of freedom and thus is roughly static compared to the fluctuations of the lattice, yielding virtually the same conductivity as the dc conductivity and manifesting as a conductivity plateau below the Debye frequency. Nevertheless, there is still a generic trend similar to the frozen potential approximation: the higher temperature yields a more substantial DDP, suggesting that the transiently localized states are at play in both cases. This tendency is also evident in Fig. 4 where the increase in temperature moves the DDP to higher absorption frequencies while broadening the peak at the same time.

The physical picture behind the observed DDP evolution is that the increase in temperature has a twofold effect. First, it yields stronger spatially localized, transient electronic states at the Fermi energy (shift to higher frequencies); electrons either residing in local potential wells (frozen) or nesting in instantaneous potential pockets (dynamic). These local wells or nests become more energetically confining as the deformation potential strengthens with the rising temperature. As a result, the location of the DDP roughly scales like $\hbar\omega_p \sim V_{\text{rms}}$, which defines the fitting illustrated by the colored dashed curves

in the upper panel of Fig. 4 [83]. In general, the peak location migrates like $\hbar\omega_p \sim (k_B T)^{3/2}$ at low temperatures $T \ll T_D$ and $\hbar\omega_p \sim (k_B T)^{1/2}$ at high temperatures $T \gg T_D$. In addition, the presence of eigenstate localization caused by the frozen lattice disorder is known to result in band tails in the density of states [47] that has later shown to persist even under quantum-acoustical lattice dynamics [84].

On the other hand, a higher temperature permits a wider energy window for electronic transitions to occur (the broadening of the peak). Whereas the transition element between the (momentarily) localized states dictates the location of DDP, the width is instead determined by the broadening function characterizing the energetically allowed transition. As indicated by the black dashed line in the lower panel of Fig. 4, the widths of the DDP behave roughly as $\hbar\Delta\omega_p \sim k_B T$ that is interestingly more accurate in the case of the dynamical potential landscape. The quantum-acoustical DDP is thus intimately connected to the ambiguous Planckian timescale $\hbar/k_B T$ that underpins the linear-in-temperature resistivity exhibited by numerous families of bad and strange metals (for comparison, see Ref. [82]). In addition, this observed correlation between the width of the DDP and Planckian behavior supports the prospect of the near-universal transport by transient dynamics reported in Refs. [47,58].

In the quantum-acoustic DDP scheme, there are no extrinsic sources, such as defects or impurities, which could also generate or enhance a shift in optical conductivity (see, e.g., Refs. [85–87]). In other words, the disorder at the origin of our DDP is *self-generated*, arising from the existence of thermally fluctuating lattice degrees of freedom that significantly affect the charge carrier dynamics. In particular, our DDP gives a unique temperature-dependent fingerprint, clearly distinguishing it from an impurity-induced DDP. The general trend of a DDP seen in Fig. 3 qualitatively agrees with experimental observations [88], also supporting the scaling behavior of the quantum-acoustical DDP illustrated in Fig. 4 [89]. Noteworthy, the transient dynamics driving the birth of an acoustical DPP resides within a dynamical regime of nonperturbative and coherent electron-lattice motion, thus lying outside the reach of the conventional perturbative or Boltzmann transport methods (see Ref. [47]). In fact, many bad and strange metals are on the verge of a transient localization and/or have strong electron-phonon coupling [1,46].

Moreover, alongside the DDP formation and Planckian resistivity, the deformation potential perspective offers a natural pathway for charge carriers in strange metals to cross the MIR bound with impunity at high temperatures [13,14], as already asserted in Ref. [47]. We explicitly demonstrated the violation of the MIR limit with quantum acoustics in another paper [58]. Our approach also carries the potential to enlighten the perplexing phenomenon of pseudogaps [4–8] and charge density waves [9–12]. In particular, we see that when electron motion strongly

couples and synchronizes with low-energy lattice vibration modes, it creates a favorable environment for incommensurate charge density order. Likewise, a similar resonance promoted by the deformation potential could result in temperature-dependent pseudogaps, i.e., a substantial suppression in the density of the low-energy excitations, which eventually melt away leaving the pseudogap phase regime. We aim to study these considerations in future research.

In conclusion, we have introduced the phenomenon of quantum-acoustical Drude peak displacement, which involves the temperature-dependent shift and broadening of the optical conductivity peak to finite frequencies, demonstrated here for three archetypal strange metals. Overall, the coherent state picture of lattice vibrations, which has always been at one's disposal but not utilized, provides a fresh perspective on the investigation of the mysteries of bad and strange metals. The manifested shift in perspective simply comes from the coherent state limit of quantum acoustics.

We are thankful for the useful discussions with D. Kim, B. Halperin, S. Das Sarma, J. H. Miller Jr, R. L. Greene, R. Lobo, and A. P. Mackenzie. Furthermore, J. K.-R. thanks the Emil Aaltonen Foundation, Vaisala Foundation, and the Oskar Huttunen Foundation, and A. M. G. thanks the Harvard Quantum Initiative for financial support.

*joonas_keskirahkonen@fas.harvard.edu

- [1] C. M. Varma, Colloquium: Linear in temperature resistivity and associated mysteries including high temperature superconductivity, *Rev. Mod. Phys.* **92**, 031001 (2020).
- [2] W. E. Pickett, Colloquium: Room temperature superconductivity: The roles of theory and materials design, *Rev. Mod. Phys.* **95**, 021001 (2023).
- [3] X. Zhou, W.-S. Lee, M. Imada, N. Trivedi, P. Phillips, H.-Y. Kee, P. Törmä, and M. Eremets, High-temperature superconductivity, *Nat. Rev. Phys.* **3**, 462 (2021).
- [4] A. Millis, Gaps and our understanding, *Science* **314**, 1888 (2006).
- [5] T. Timusk and B. Statt, The pseudogap in high-temperature superconductors: An experimental survey, *Rep. Prog. Phys.* **62**, 61 (1999).
- [6] A. Damascelli, Z. Hussain, and Z.-X. Shen, Angle-resolved photoemission studies of the cuprate superconductors, *Rev. Mod. Phys.* **75**, 473 (2003).
- [7] D. N. Basov and T. Timusk, Electrodynamics of high- T_c superconductors, *Rev. Mod. Phys.* **77**, 721 (2005).
- [8] Ø. Fischer, M. Kugler, I. Maggio-Aprile, C. Berthod, and C. Renner, Scanning tunneling spectroscopy of high-temperature superconductors, *Rev. Mod. Phys.* **79**, 353 (2007).
- [9] G. Grüner, The dynamics of charge-density waves, *Rev. Mod. Phys.* **60**, 1129 (1988).
- [10] T. Wu, H. Mayaffre, S. Krämer, M. Horvatić, C. Berthier, W. Hardy, R. Liang, D. Bonn, and M.-H. Julien, Magnetic-field-induced charge-stripe order in the high-temperature superconductor $\text{YBa}_2\text{Cu}_3\text{O}_y$, *Nature (London)* **477**, 191 (2011).
- [11] J. Chang, E. Blackburn, A. Holmes, N. B. Christensen, J. Larsen, J. Mesot, R. Liang, D. Bonn, W. Hardy, A. Watenphul *et al.*, Direct observation of competition between superconductivity and charge density wave order in $\text{YBa}_2\text{Cu}_3\text{O}_{6.67}$, *Nat. Phys.* **8**, 871 (2012).
- [12] G. Ghiringhelli, M. Le Tacon, M. Minola, S. Blanco-Canosa, C. Mazzoli, N. Brookes, G. De Luca, A. Frano, D. Hawthorn, F. He *et al.*, Long-range incommensurate charge fluctuations in $(\text{Y,Nd})\text{Ba}_2\text{Cu}_3\text{O}_{(6+x)}$, *Science* **337**, 821 (2012).
- [13] N. E. Hussey, K. Takenaka, and H. Takagi, Universality of the Mott-Ioffe-Regel limit in metals, *Philos. Mag.* **84**, 2847 (2004).
- [14] O. Gunnarsson, M. Calandra, and J. E. Han, Colloquium: Saturation of electrical resistivity, *Rev. Mod. Phys.* **75**, 1085 (2003).
- [15] N. E. Hussey, R. A. Cooper, X. Xu, Y. Wang, I. Mouzopoulou, B. Vignolle, and C. Proust, Dichotomy in the T -linear resistivity in hole-doped cuprates, *Phil. Trans. R. Soc. A* **369**, 1626 (2011).
- [16] K. Hashimoto, K. Cho, T. Shibauchi, S. Kasahara, Y. Mizukami, R. Katsumata, Y. Tsuruhara, T. Terashima, H. Ikeda, M. A. Tanatar, H. Kitano, N. Salovich, R. W. Giannetta, P. Walmsley, A. Carrington, R. Prozorov, and Y. Matsuda, A sharp peak of the zero-temperature penetration depth at optimal composition in $\text{BaFe}_2(\text{As}_{1-x}\text{P}_x)_2$, *Science* **336**, 1554 (2012).
- [17] J. A. N. Bruin, H. Sakai, R. S. Perry, and A. P. Mackenzie, Similarity of scattering rates in metals showing T -linear resistivity, *Science* **339**, 804 (2013).
- [18] A. Legros, S. Benhabib, W. Tabis, F. Laliberté, M. Dion, M. Lizaire, B. Vignolle, D. Vignolles, H. Raffy, Z. Z. Li, P. Auban-Senzier, N. Doiron-Leyraud, P. Fournier, D. Colson, L. Taillefer, and C. Proust, Universal T -linear resistivity and Planckian dissipation in overdoped cuprates, *Nat. Phys.* **15**, 142 (2018).
- [19] H. Polshyn, M. Yankowitz, S. Chen, Y. Zhang, K. Watanabe, T. Taniguchi, C. R. Dean, and A. F. Young, Large linear-in-temperature resistivity in twisted bilayer graphene, *Nat. Phys.* **15**, 1011 (2019).
- [20] G. Grissonnanche, Y. Fang, A. Legros, S. Verret, F. Laliberté, C. Collignon, J. Zhou, D. Graf, P. A. Goddard, L. Taillefer, and B. J. Ramshaw, Linear-in temperature resistivity from an isotropic Planckian scattering rate, *Nature (London)* **595**, 667 (2021).
- [21] Y. Chu, L. Liu, C. Shen, J. Tian, J. Tang, Y. Zhao, J. Liu, Y. Yuan, Y. Ji, R. Yang, K. Watanabe, T. Taniguchi, D. Shi, F. Wu, W. Yang, and G. Zhang, Temperature-linear resistivity in twisted double bilayer graphene, *Phys. Rev. B* **106**, 035107 (2022).
- [22] S. A. Hartnoll and A. P. Mackenzie, Colloquium: Planckian dissipation in metals, *Rev. Mod. Phys.* **94**, 041002 (2022).
- [23] P. Kostic, Y. Okada, N. C. Collins, Z. Schlesinger, J. W. Reiner, L. Klein, A. Kapitulnik, T. H. Geballe, and M. R. Beasley, Non-Fermi-liquid behavior of SrRuO_3 : Evidence from infrared conductivity, *Phys. Rev. Lett.* **81**, 2498 (1998).
- [24] Y. S. Lee, J. Yu, J. S. Lee, T. W. Noh, T.-H. Gimm, H.-Y. Choi, and C. B. Eom, Non-Fermi liquid behavior and

- scaling of the low-frequency suppression in the optical conductivity spectra of CaRuO_3 , *Phys. Rev. B* **66**, 041104(R) (2002).
- [25] C. Bernhard, A. V. Boris, N. N. Kovaleva, G. Khaliullin, A. V. Pimenov, L. Yu, D. P. Chen, C. T. Lin, and B. Keimer, Charge ordering and magnetopolarons in $\text{Na}_{0.82}\text{CoO}_2$, *Phys. Rev. Lett.* **93**, 167003 (2004).
- [26] A. A. Tsvetkov, J. Schützmann, J. I. Gorina, G. A. Kaljushnaia, and D. van der Marel, In-plane optical response of $\text{Bi}_2\text{Sr}_2\text{CuO}_6$, *Phys. Rev. B* **55**, 14152 (1997).
- [27] K. Takenaka, J. Nohara, R. Shiozaki, and S. Sugai, Incoherent charge dynamics of $\text{La}_{2-x}\text{Sr}_x\text{CuO}_4$: Dynamical localization and resistivity saturation, *Phys. Rev. B* **68**, 134501 (2003).
- [28] T. Osafune, N. Motoyama, H. Eisaki, S. Uchida, and S. Tajima, Pseudogap and collective mode in the optical conductivity spectra of hole-doped ladders in $\text{Sr}_{14-x}\text{Ca}_x\text{Cu}_{24}\text{O}_{41}$, *Phys. Rev. Lett.* **82**, 1313 (1999).
- [29] M. J. Rozenberg, G. Kotliar, H. Kajueter, G. A. Thomas, D. H. Rapkine, J. M. Honig, and P. Metcalf, Optical conductivity in Mott-Hubbard systems, *Phys. Rev. Lett.* **75**, 105 (1995).
- [30] P. E. Jönsson, K. Takenaka, S. Niitaka, T. Sasagawa, S. Sugai, and H. Takagi, Correlation-driven heavy-fermion formation in LiV_2O_4 , *Phys. Rev. Lett.* **99**, 167402 (2007).
- [31] K. Takenaka, Y. Sawaki, and S. Sugai, Incoherent-to-coherent crossover of optical spectra in $\text{La}_{0.825}\text{Sr}_{0.175}\text{MnO}_3$: temperature-dependent reflectivity spectra measured on cleaved surfaces, *Phys. Rev. B* **60**, 13011 (1999).
- [32] K. Takenaka, R. Shiozaki, and S. Sugai, Charge dynamics of a double-exchange ferromagnet $\text{La}_{1-x}\text{Sr}_x\text{MnO}_3$, *Phys. Rev. B* **65**, 184436 (2002).
- [33] J. Dong, J. L. Musfeldt, J. A. Schlueter, J. M. Williams, P. G. Nixon, R. W. Winter, and G. L. Gard, Optical properties of $\beta'' - (\text{ET})_2\text{SF}_5\text{CH}_2\text{CF}_2\text{SO}_3$: A layered molecular superconductor with large discrete counterions, *Phys. Rev. B* **60**, 4342 (1999).
- [34] K. Takenaka, M. Tamura, N. Tajima, H. Takagi, J. Nohara, and S. Sugai, Collapse of coherent quasiparticle states in $\theta - (\text{BEDT} - \text{TTF})_2\text{I}_3$ observed by optical spectroscopy, *Phys. Rev. Lett.* **95**, 227801 (2005).
- [35] N. L. Wang, P. Zheng, D. Wu, Y. C. Ma, T. Xiang, R. Y. Jin, and D. Mandrus, Infrared probe of the electronic structure and charge dynamics of $\text{Na}_{0.7}\text{CoO}_2$, *Phys. Rev. Lett.* **93**, 237007 (2004).
- [36] R. Jaramillo, S. D. Ha, D. Silevitch, and S. Ramanathan, Origins of bad-metal conductivity and the insulator-metal transition in the rare-earth nickelates, *Nat. Phys.* **10**, 304 (2014).
- [37] J. Hwang, T. Timusk, and G. Gu, Doping dependent optical properties of $\text{Bi}_2\text{Sr}_2\text{CaCu}_2\text{O}_{8+\delta}$, *J. Condens. Matter Phys.* **19**, 125208 (2007).
- [38] P. A. Lee and T. V. Ramakrishnan, Disordered electronic systems, *Rev. Mod. Phys.* **57**, 287 (1985).
- [39] N. V. Smith, Classical generalization of the Drude formula for the optical conductivity, *Phys. Rev. B* **64**, 155106 (2001).
- [40] M. Kaveh and N. Mott, Universal dependences of the conductivity of metallic disordered systems on temperature, magnetic field and frequency, *J. Phys. C* **15**, L707 (1982).
- [41] S. Fratini and S. Ciuchi, Displaced Drude peak and bad metal from the interaction with slow fluctuations, *SciPost Phys.* **11**, 39 (2021).
- [42] A. Pustogow, Y. Saito, A. Löhle, M. S. Alonso, A. Kawamoto, V. Dobrosavljević, M. Dressel, and S. Fratini, Rise and fall of Landau's quasiparticles while approaching the mott transition, *Nat. Commun.* **12**, 1571 (2021).
- [43] S. Caprara, C. Di Castro, S. Fratini, and M. Grilli, Anomalous optical absorption in the normal state of overdoped cuprates near the charge-ordering instability, *Phys. Rev. Lett.* **88**, 147001 (2002).
- [44] L. V. Delacrétaz, B. Goutéraux, S. A. Hartnoll, and A. Karlsson, Bad metals from fluctuating density waves, *SciPost Phys.* **3**, 025 (2017).
- [45] D. N. Basov, R. D. Averitt, D. van der Marel, M. Dressel, and K. Haule, Electrodynamics of correlated electron materials, *Rev. Mod. Phys.* **83**, 471 (2011).
- [46] A. Lanzara, P. V. Bogdanov, X. J. Zhou, S. A. Kellar, D. L. Feng, E. D. Lu, T. Yoshida, H. Eisaki, A. Fujimori, K. Kishio, J.-I. Shimoyama, T. Noda, S. Uchida, Z. Hussain, and Z.-X. Shen, Evidence for ubiquitous strong electron-phonon coupling in high-temperature superconductors, *Nature (London)* **412**, 510 (2001).
- [47] D. Kim, A. Aydin, A. Daza, K. N. Avanaki, J. Keski-Rahkonen, and E. J. Heller, Coherent charge carrier dynamics in the presence of thermal lattice vibrations, *Phys. Rev. B* **106**, 054311 (2022).
- [48] A. A. Patel, H. Guo, I. Esterlis, and S. Sachdev, Universal theory of strange metals from spatially random interactions, *Science* **381**, 790 (2023).
- [49] A. Gogolin, V. Mel'nikov, and E. Rashba, Conductivity in a disordered one-dimensional system induced by electron-phonon interaction, *Sov. J. Exp. Theor. Phys.* **42**, 168 (1975).
- [50] E. Rashba, A. Gogolin, and V. Mel'nikov, *In Organic Conductors and Semiconductors*, Lecture Notes in Physics Vol. 65 (Springer Berlin Heidelberg, 1977).
- [51] D. J. Thouless, Maximum metallic resistance in thin wires, *Phys. Rev. Lett.* **39**, 1167 (1977).
- [52] E. Abrahams, *50 Years of Anderson Localization* (World Scientific, Singapore, 2010), Vol. 24.
- [53] P. W. Anderson, Absence of diffusion in certain random lattices, *Phys. Rev.* **109**, 1492 (1958).
- [54] D. Di Sante, S. Fratini, V. Dobrosavljević, and S. Ciuchi, Disorder-driven metal-insulator transitions in deformable lattices, *Phys. Rev. Lett.* **118**, 036602 (2017).
- [55] S. Fratini, D. Mayou, and S. Ciuchi, The transient localization scenario for charge transport in crystalline organic materials, *Adv. Funct. Mater.* **26**, 2292 (2016).
- [56] A. Troisi and G. Orlandi, Charge-transport regime of crystalline organic semiconductors: Diffusion limited by thermal off-diagonal electronic disorder, *Phys. Rev. Lett.* **96**, 086601 (2006).
- [57] A. Lacroix, G. T. de Laissardière, P. Quémerais, J.-P. Julien, and D. Mayou, Modeling of electronic mobilities in halide perovskites: Adiabatic quantum localization scenario, *Phys. Rev. Lett.* **124**, 196601 (2020).
- [58] A. Aydin, J. Keski-Rahkonen, and E. J. Heller, Quantum acoustics spawns Planckian resistivity, [arXiv:2303.06077](https://arxiv.org/abs/2303.06077).
- [59] S. Sachdev, Quantum phase transitions, *Phys. World* **12**, 33 (1999).

- [60] D. Chowdhury, A. Georges, O. Parcollet, and S. Sachdev, Sachdev-Ye-Kitaev models and beyond: Window into non-Fermi liquids, *Rev. Mod. Phys.* **94**, 035004 (2022).
- [61] S. Sachdev, *Quantum Phases of Matter* (Cambridge University Press, Cambridge, England, 2023).
- [62] H. Fröhlich, Electrons in lattice fields, *Adv. Phys.* **3**, 325 (1954).
- [63] H. Fröhlich and N. F. Mott, Theory of electrical breakdown in ionic crystals, *Proc. R. Soc. A* **160**, 230 (1937).
- [64] G. D. Mahan, *Many-Particle Physics* (Springer Science & Business Media, New York, 2000).
- [65] See Supplemental Material at <http://link.aps.org/supplemental/10.1103/PhysRevLett.132.186303> including the Refs. [47,58] for Sec. I: a short derivation of the deformation potential from the Hamiltonian and explaining its key features; a more complete discussion on the coherent state formalism in the context of lattice vibrations; and on the deformation potential, which can be found in Ref. [47], and its relation to quantum transport in Ref. [58]. Section II: the material properties, which includes Refs. [66–74]. Moreover, these parameters are in line with Ref. [58]. Section III: a detailed description about the Kubo calculations carried out in the case of a frozen potential. In the nutshell, we first numerically determine the eigenstates of an ensemble of the frozen deformation potential, and then employ them to compute the optical conductivity via the Kubo formula. Section IV: explicating the computation of the optical conductivity within the Kubo formulation in the case of the dynamical deformation potential. In summary, we take the already resolved eigenstates, and let them evolve under the time-dependent deformation potential defined in Eq. (2). By computing the velocity autocorrelation for all time steps, we numerically determine the optical conductivity in the case of a dynamical lattice disorder field within the Kubo formulation.
- [66] I. Bozovic, G. Logvenov, I. Belca, B. Narimbetov, and I. Sveklo, Epitaxial strain and superconductivity in $\text{La}_{2-x}\text{Sr}_x\text{CuO}_4$ thin films, *Phys. Rev. Lett.* **89**, 107001 (2002).
- [67] D. Ross *et al.*, A determination of the variation in the lattice parameters of $\text{Bi}_2\text{Sr}_2\text{CaCu}_2\text{O}_{8+x}$ (Bi-2212) as a function of temperature and oxygen content, *Physica (Amsterdam)* **425C**, 130 (2005).
- [68] H. Ledbetter, M. Lei, and S. Kim, Elastic constants, Debye temperatures, and electron-phonon parameters of superconducting cuprates and related oxides, *Phase Transitions* **23**, 61 (1990).
- [69] J. L. Cohn, C. K. Lowe-Ma, and T. A. Vanderah, Anomalous phonon damping and thermal conductivity in insulating cuprates, *Phys. Rev. B* **52**, R13134 (1995).
- [70] C. Walsh, M. Charlebois, P. Sémon, G. Sordi, and A.-M. S. Tremblay, Prediction of anomalies in the velocity of sound for the pseudogap of hole-doped cuprates, *Phys. Rev. B* **106**, 235134 (2022).
- [71] W. J. Padilla, Y. S. Lee, M. Dumm, G. Blumberg, S. Ono, K. Segawa, S. Komiya, Y. Ando, and D. N. Basov, Constant effective mass across the phase diagram of high- T_c cuprates, *Phys. Rev. B* **72**, 060511(R) (2005).
- [72] A. Legros, S. Benhabib, W. Tabis, F. Laliberté, M. Dion, M. Lizaire, B. Vignolle, D. Vignolles, H. Raffy, Z. Li *et al.*, Universal T -linear resistivity and Planckian dissipation in overdoped cuprates, *Nat. Phys.* **15**, 142 (2019).
- [73] J. A. N. Bruin, H. Sakai, R. S. Perry, and A. Mackenzie, Similarity of scattering rates in metals showing t -linear resistivity, *Science* **339**, 804 (2013).
- [74] G. Grissonnanche, Y. Fang, A. Legros, S. Verret, F. Laliberté, C. Collignon, J. Zhou, D. Graf, P. A. Goddard, L. Taillefer, and B. J. Ramshaw, Linear-in temperature resistivity from an isotropic Planckian scattering rate, *Nature (London)* **595**, 667 (2021).
- [75] N. Ashcroft and N. Mermin, *Solid State Physics*, HRW International Editions (Rinehart and Winston, Holt, New York, 1976).
- [76] F. Bloch, Zum elektrischen widerstandsgesetz bei tiefen temperaturen, *Z. Phys.* **59**, 208 (1930).
- [77] E. Grüneisen, The temperature dependence of the electrical resistance of pure metals, *Ann. Phys. (Leipzig)* **16**, 530 (1933).
- [78] R. H. Brown and R. Q. Twiss, Interferometry of the intensity fluctuations in light. I. Basic theory: The correlation between photons in coherent beams of radiation, *Proc. R. Soc. A* **242**, 300 (1957).
- [79] R. J. Glauber, Coherent and incoherent states of the radiation field, *Phys. Rev.* **131**, 2766 (1963).
- [80] W. Shockley and J. Bardeen, Energy bands and mobilities in monatomic semiconductors, *Phys. Rev.* **77**, 407 (1950).
- [81] J. Bardeen and W. Shockley, Deformation potentials and mobilities in non-polar crystals, *Phys. Rev.* **80**, 72 (1950).
- [82] L. V. Delacrétaz, B. Goutéraux, S. A. Hartnoll, and A. Karlsson, Bad metals from fluctuating density waves, *SciPost Phys.* **3**, 025 (2017).
- [83] More specifically, we define the peak location of a displaced Drude peak as $\hbar\omega_p = a + bV_{\text{rms}}$, where a and b are fitting parameters, and the temperature dependence is included in the root mean square of the deformation potential V_{rms} that is explicitly presented in Supplemental Material [65].
- [84] D. Kim and B. I. Halperin, Low-energy tail of the spectral density for a particle interacting with a quantum phonon bath, *Phys. Rev. B* **107**, 224311 (2023).
- [85] D. N. Basov, B. Dabrowski, and T. Timusk, Infrared probe of transition from superconductor to nonmetal in $\text{YBa}_2(\text{Cu}_{1-x}\text{Zn}_x)_4\text{O}_8$, *Phys. Rev. Lett.* **81**, 2132 (1998).
- [86] N. L. Wang, S. Tajima, A. I. Rykov, and K. Tomimoto, Zn-substitution effects on the optical conductivity in $\text{YBa}_2\text{Cu}_3\text{O}_{7-\delta}$ crystals: Strong pair breaking and reduction of in-plane anisotropy, *Phys. Rev. B* **57**, R11081 (1998).
- [87] D. N. Basov, A. V. Puchkov, R. A. Hughes, T. Strach, J. Preston, T. Timusk, D. A. Bonn, R. Liang, and W. N. Hardy, Disorder and superconducting-state conductivity of single crystals of $\text{YBa}_2\text{Cu}_3\text{O}_{6.95}$, *Phys. Rev. B* **49**, 12165 (1994).
- [88] There is a growing multitude of experimental evidence on the emergence of a displaced Drude peak in several strange metals, which widens and moves toward higher frequencies with increasing temperature; see, e.g., K. Takenaka, R. Shiozaki, S. Okuyama, J. Nohara, A. Osuka, Y. Takayanagi, and S. Sugai, Coherent-to-incoherent crossover in the optical conductivity of $\text{La}_{2-x}\text{Sr}_x\text{CuO}_4$: Charge dynamics of a bad metal, *Phys. Rev. B* **65**, 092405 (2002); A. F. Santander-Syro, R. P. S. M. Lobo, N. Bontemps,

- Z. Konstantinovic, Z. Z. Li, and H. Raffy, Absence of a Loss of In-Plane Infrared Spectral Weight in the Pseudogap Regime of $\text{Bi}_2\text{Sr}_2\text{CaCu}_2\text{O}_{8+\delta}$, *Phys. Rev. Lett.* **88**, 097005 (2002); C. C. Homes, R. P. S. M. Lobo, P. Fournier, A. Zimmers, and R. L. Greene, Optical determination of the superconducting energy gap in electron-doped $\text{Pr}_{1.85}\text{Ce}_{0.15}\text{CuO}$, *Phys. Rev. B* **74**, 214515 (2006); J. P. Falck, A. Levy, M. A. Kastner, and R. J. Birgeneau, Optical excitation of polaronic impurities in $\text{La}_2\text{CuO}_{4+y}$, *Phys. Rev. B* **48**, 4043 (1993); J. P. Falck, A. Levy, M. A. Kastner, and R. J. Birgeneau, *Phys. Rev. B* **48**, 4043 (1993).
- [89] The experimental datasets collected in Refs. [41,82] reveal a prominent role of thermal fluctuations as expected within the present framework. As reported in Ref. [41], the temperature dependence of the DDP peak in various material follows $\hbar\omega_p \propto T^\alpha$, where $0.5 \leq \alpha \leq 1.5$. Moreover, in various classes of strange or bad metals, the width of the peak is experimentally found to lie at the Planckian bound ($\hbar\Delta\omega_p \approx k_B T$), as collectively presented in Ref. [82]. Both of these experimental features are in agreement of the theory of the quantum-acoustical DDP.